ELSEVIER

Journal of Hazardous Materials B83 (2001) 243–254

Journal of Hazardous Materials

www.elsevier.nl/locate/jhazmat

Effects of pH on dechlorination of trichloroethylene by zero-valent iron

Jiann-Long Chen [a,*], Souhail R. Al-Abed [b], James A. Ryan [b], Zhenbin Li [b]

[a] *Department of Civil and Environmental Engineering, North Carolina Agricultural and Technical State University, 1601 East Market Street, Greensboro, NC 27411, USA*

[b] *National Risk Management Research Laboratory, US EPA, Cincinnati, OH 45268, USA*

Received 6 November 2000; received in revised form 12 February 2001; accepted 19 February 2001

Abstract

The surface normalized reaction rate constants (k_{sa}) of trichloroethylene (TCE) and zero-valent iron (ZVI) were quantified in batch reactors at pH values between 1.7 and 10. The k_{sa} of TCE linearly decreased from 0.044 to 0.009 l/h m^2 between pH 3.8 and 8.0, whereas the k_{sa} at pH 1.7 was more than an order higher than that at pH 3.8. The degradation of TCE was not observed at pH values of 9 and 10. The k_{sa} of iron corrosion linearly decreased from 0.092 to 0.018 l/h m^2 between pH 4.9 and 9.8, whereas it is significantly higher at pH 1.7 and 3.8. The k_{sa} of TCE was 30–300 times higher than those reported in literature. The difference can be attributed to the pH effects and precipitation of iron hydroxide. The k_{sa} of TCE degradation and iron corrosion at a head space of 6 and 10 ml were about twice of those at zero head space. The effect was attributed to the formation of hydrogen bubbles on ZVI, which hindered the transport the TCE between the solution and reaction sites on ZVI. The optimal TCE degradation rate was achieved at a pH of 4.9. This suggests that lowering solution pH might not expedite the degradation rate of TCE by ZVI as it also caused faster disappearance of ZVI, and hence decreased the ZVI surface concentration.

Keywords: Zero-valent iron (ZVI); Trichloroethylene (TCE); Iron corrosion; Chlorinated organics

1. Introduction

ZVI has been shown to be an effective material to remediate groundwater contaminated with chlorinated organic compounds [1–6]. As ZVI can be obtained in bulk quantity with little cost, it was used as the medium in reactive barrier walls and showed encouraging performance results [7]. Among the chlorinated organic compounds, carbon tetrachloride

* Corresponding author. Tel.: +1-336-334-7737; fax: +1-336-334-7667.
E-mail address: chenjl@ncat.edu (J.-L. Chen).

0304-3894/01/$ – see front matter
PII: S0304-3894(01)00193-5

(CT) and TCE are more thoroughly studied than other compounds. Gillham and O'Hannesin [1], using the results of CT reduction by ZVI, concluded that the degradation process is a simple reductive dechlorination, with ZVI serving as the electron donor. They demonstrated that CT needs to directly contact the metal surface to be dechlorinated. The results obtained by Matheson and Tratnyek [2] also suggest that reductive dechlorination of CT occurred at the iron surface. Matheson and Tratnyek [2] and Muftikian et al. [3] proposed that the dechlorination process is a consequence of direct oxidative corrosion of the iron by TCE. The reaction can be written as Eq. (1) stoichiometrically.

$$Fe^0 \rightarrow Fe^{2+} + 2e^-, \qquad C_2HCl_3 + 3H^+ + 6e^- \overset{\text{iron surface}}{\rightarrow} C_2H_4 + 3Cl^- \tag{1}$$

Between the final products and TCE, there are several reactions steps involved [8]. First, TCE is diffused through the solution to the metal surface and adsorbed to a favorable reaction site. Then, electrons are transferred from the ZVI to the TCE, producing intermediate products, such as dichloroethylene (DCE) isomers, chloroacetylene, and vinyl chloride (VC). The intermediate products are sequentially transformed to less chlorinated compounds on the surface. Finally, some of the intermediate and final products diffuse from the ZVI surface to the solution.

The kinetics of TCE reduction by ZVI is generally assumed a pseudo-first-order reaction with respect to the aqueous TCE concentration [5,8,9]. As the reduction occurs at the surface of ZVI, the surface area concentration in the solution was found to be the most important parameter in determining the reaction rate. Accordingly, the relationship between TCE concentration and time can be written as Eq. (2).

$$\ln\left(\frac{C(t)}{C_0}\right) = -k_{\text{sa,TCE}}\,\rho_{\text{a}}(t)t \tag{2}$$

where $C(t)$ is the TCE concentration (μM), C_0 the initial TCE concentration (μM), $k_{\text{sa,TCE}}$ the surface normalized reaction rate constant (l/h m^2), $\rho_{\text{a}}(t)$ the surface area concentration of ZVI in solution (m^2/l), and t is the time (h).

pH is another parameter that affects the reduction rates of chlorinated organic compounds by ZVI. Matheson and Tratnyek [2] showed that the relationship between k_{sa} for CT decreases approximately linearly with pH between pH 5.5 and 10. Their results also showed that although the pH spanned five orders of magnitude, the k_{sa} for CT decreased only by 80%. Deng et al. [6] showed that the k_{sa} for VC changed less than an order of magnitude between pH 6 and 10. However, the relationship between the k_{sa} for VC and pH is nonlinear.

The other reaction that concurrently occurs with Eq. (1) is the corrosion of ZVI, which produces hydrogen gas and hydroxyl ion (Eq. (3)).

$$Fe^0 \rightarrow Fe^{2+} + 2e^-, \qquad 2H_2O + 2e^- \overset{\text{surface}}{\rightarrow} 2OH^- + H_2(g) \tag{3}$$

Eq. (3) suggests that iron corrosion could have detrimental effect on the reduction of TCE as water competes with TCE for the electrons from ZVI. At elevated pH, the ferrous and hydroxyl ions form ferrous hydroxide and precipitate. The precipitation of ferrous hydroxide on the surface of ZVI could hinder the transport of the TCE and block the reactive sites on ZVI, and hence decrease the overall reaction rate [10]. As the solubility of ferrous

hydroxide is strongly dependent on pH, amount of ferrous hydroxide on the surface of ZVI is controlled by the pH. Therefore, pH could affect the rate of iron corrosion and the amount of precipitation on ZVI surface. Both could affect the TCE degradation rate by ZVI. The objectives of this study are: (1) to characterize the effect of pH on TCE degradation using ZVI; (2) quantify the kinetics of iron corrosion, and (3) characterize the effect of pH on iron corrosion. These results will provide essential information to enhance the efficiency of the treatment scenarios where ZVI is used as the dechlorination agent.

2. Experimental setup

The rate of dechlorination of TCE by ZVI at eight different pH values (1.7, 4, 5, 6, 7, 8, 9, and 10) were studied in sets of experiments, each includes 33 batch reactors (26.0 ± 0.3 ml serum bottles). For a set of experiment, 15 batch reactors filled with 20 ml of the same solution matrix (i.e. same pH buffer) were loaded with 50 ± 2 mg of iron particles (Fisher Scientific, finer than 100 mesh). The reactors were crimp-sealed and spiked with TCE (Fisher Scientific, ACS grade) stock solution so that the initial concentration was approximately 0.5 mM (65 ppm). The surface area density of the ZVI measured with a surface area analyzer (Micromeritics, Gemini III 2375) was 0.077 m^2/g. This was comparable to the 0.091 m^2/g value measured by Su and Puls [8]. In addition, 18 reactors filled with the same contents as the test reactors with no ZVI added were used as the control. The initial TCE concentrations at all pH values except 1.7 were measured using three of the control reactors, which were shaken for 3 h at 400 rpm on a rotational shaker. The initial TCE concentrations at pH 1.7 was measured immediately after the TCE was added to the solution as the loss of ZVI at this pH is substantial in 3 h. The rest of the test and control reactors were stored in an anaerobic glove box and analyzed (triplicate samples) for pH, concentrations of TCE and total iron, and head space pressure at several different reaction periods. The sampling periods varied with pH as at higher pH values, longer time was needed to observe the TCE degradation and iron corrosion. The average results from the triplicate measurements were used in determining the surface normalized reaction rate constants of TCE reduction and iron corrosion.

The buffer solutions were phosphate-based, i.e. different ratio of H_3PO_4, NaH_2PO_4, Na_2HPO_4, and Na_3PO_4 were mixed to obtain the desired pH. The total phosphate concentrations ranged from 0.1 to 0.5 M depending on the pH of each set of experiment. The solution was de-aired by purging ultra-high-purity grade nitrogen gas through it for no less than 4 h.

The initial ZVI concentration was approximately 2.5 mg/ml, which was smaller than the values between 250 and 333 mg/ml typically found in other experiments [1,2,8]. This is because in our preliminary tests higher iron loading produced more hydroxyl ions that exhausted the buffer capacity of the solution and caused the pH to significantly increase. The preliminary tests also showed iron phosphate precipitated when more ferrous irons were produced in the solution.

To prevent ferrous iron from forming ferrous phosphate precipitate, di-sodium ethylenediaminetetraacetic acid (EDTA, 0.05 M) was added to the solutions at pH values higher than 4 so that all the ferrous iron stayed dissolved and could be detected. EDTA was not added in experiment with pH values lower than 4 since ferrous phosphate is more soluble, whereas EDTA is scarcely soluble under such conditions. The effect of EDTA on the rate constants of

TCE and iron corrosion is assumed minor compared to that of pH. We do acknowledge that the addition of chelating agents such as EDTA has been shown to increase the dissolved iron concentration [5], whereas its effect on the VC and CT reduction by ZVI is minimum [2,5]. In spite of the effect of EDTA on iron corrosion, it is of critical importance to prevent any precipitation of iron from forming on the surface of ZVI to characterize the effect of pH on the rate constants of TCE reduction and iron corrosion. Without adding EDTA, the results we obtained would be ambiguous as the variations in rate constants of TCE reduction and iron corrosion could be caused by the pH change as well as by the precipitation of ferrous phosphate/hydroxide.

3. Analytical methods

At each sampling period, the conditions and content of triplicate bottles were monitored and analyzed according to the following procedures and methods.

3.1. Head space pressure

Head space pressure was measured by penetrating the septum with a needle pressure gauge (Supelco 2–99 psi in 0.5 psi increments). The head space pressure was used to estimated the amount of hydrogen gas produced.

3.2. TCE concentration

TCE is extracted by injecting 5 ml of pure toluene into the reactor, which was then shaken on a rotary shaker at 400 rpm for 12 min. Approximately 1 ml of the toluene was withdrawn with a glass syringe and filtered through 0.2 μm. The filtered toluene was sealed in a 2 ml vial. The TCE concentrations in the toluene was analyzed with a GC(HP 5890 II)/MS (HP 5971) equipped with an autosampler (HP 7673). The injection volume was 1 μl (split injector). The column in the GC was a Supelco Vocol column (60 m; 0.25 mm i.d.). The temperature program was initially at 50°C for 5 min, ramped at 10°C/min to 180°C, and stayed at 180°C for 5 min. This method of extraction and analysis allowed us to measure all TCE in the solution matrix and minimize the effect of TCE adsorption on ZVI [11].

3.3. pH

After extraction of the TCE, approximately 10 ml of the solution was taken and measured for pH with a combination electrode (Model 81-75BN, Orion). We assumed that the extraction process did not affect the pH of the solution since toluene extracted only polar non-ionized compounds and proton remained in the solution phase rather than in the toluene phase.

3.4. Iron concentration

The total dissolve iron concentration of the solution (filtered through 0.45 μm and diluted 1–10 with Milli-Q water) was measured at the end of each set of experiment according to

EPA method 6010B using the technique of Inductively Coupled Argon Plasma (ICAP). The solution was assumed free of ZVI particles and was stored at room temperature (25°C). Since EDTA is added to the solution at pH values greater than 4 to prevent iron from precipitating as ferrous phosphate and ferrous hydroxide and the test conditions were anaerobic, the measured iron concentration was taken as the dissolved ferrous iron concentration.

4. Data analysis

The rate of the TCE degradation was determined according to Eq. (4).

$$\frac{\ln(C(t)/C_0)}{\rho_a(t)} = -k_{sa,TCE}\, t \tag{4}$$

The $k_{sa,TCE}$ was obtained by plotting $-\ln(C(t)/C_0)/\rho_a(t)$ verses t. It should be pointed out that the surface area concentration of ZVI in this study changed with time, whereas it was assumed constant in most reported experiments. The surface area concentration at each sampling period was calculated according to Eq. (5), assuming the shape of the ZVI particles are spherical and the size uniform.

$$\rho_a(t) = \rho_a(0)\left[\frac{M(t)}{M_0}\right]^{2/3} \tag{5}$$

where $\rho_a(0)$ is the initial surface concentration, M_0 the initial ZVI mass and $M(t)$ is the ZVI mass at time t. $M(t)$ is calculated by subtracting the mass of total dissolved iron (i.e. ferrous iron concentration times the solution volume) from the initial iron loading. In addition, the normalized surface reaction rate constant of iron corrosion, $k_{sa,iron}$, can be determined using Eqs. (4) and (5) by substituting the initial and subsequent ZVI concentrations for C_0 and $C(t)$, respectively.

5. Results and discussion

5.1. Iron corrosion

The corrosion of iron was observed at all pH tested except at pH 10. The color of the solution, which turns brown-to-reddish when trace amount of ferric ion is present, stayed clear throughout the test period (120–240 h) for all the experiments. This indicates that the majority of the dissolved iron species was ferrous iron and the dissolved oxygen concentration was negligible. The formation of ferrous phosphate precipitate was not observed and the color of the ZVI particles remained unchanged during the test period suggesting that ferrous iron was chelated by the EDTA. To support that ferrous iron was chelated by EDTA, we simulated the distribution of iron species using Minequl+ [12]. The conditions for the simulations were the same as the test conditions except that we assumed all the ZVI was dissolved, i.e. the worst-case scenario. The results showed no precipitation of iron and the dissolved iron were either in the form of $FeHEDTA^{-1}$ or $FeEDTA^{-2}$ at pH values greater

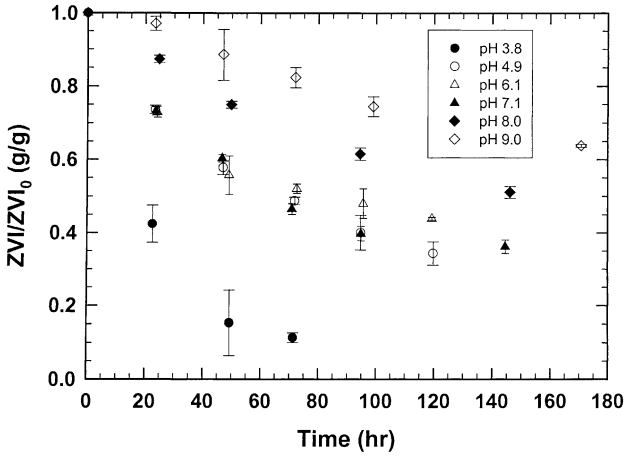

Fig. 1. Ratio of the final to the initial mass of ZVI with time at different pH.

than 3. The fraction of $FeHEDTA^{-1}$ decreased from 0.4 at pH 3 to 0.02 at pH 4.5. At pH values above 5, all the dissolved iron was in the form of $FeEDTA^{-2}$. Thus, the measured total iron concentration was taken as the ferrous iron concentration.

The average dimensionless ZVI concentration, which was the ratio of the final to the initial mass of ZVI, decreased linearly with time within the first 48 h of the test and continued to decrease at a slower rate afterward (Fig. 1). Fig. 1 also indicates that the rate of iron corrosion decreases with pH. All the data was used to plot $-\ln(C(t)/C_0)/\rho(t)$ versus t for each pH value and the slope of the regression line was taken as the surface normalized reaction rate constant (Eq. (4)). The coefficients of determination (R^2) of the regression lines are larger than 0.9 for all pH values except at pH 3.8, which yields a R^2 value of 0.79. The $k_{sa,iron}$ values decreased with pH, with the highest value of 3.58 l/h m^2 at pH 1.7. The $k_{sa,iron}$ between pH 4.9 and 9.8 shows a linear dependence on pH: decreasing from 0.061 to 0.012 l/h m^2 (Fig. 2). Linear regression analysis using the mid point of the pH ranges during each experiment yields the following relationship between $k_{sa,iron}$ and pH ($R^2 = 0.90$).

$$k_{sa,iron} = 0.125–0.012\,\text{pH} \tag{6}$$

Eq. (6) is valid only at pH values between 4.9 and 9.8. Results show that $k_{sa,iron}$ outside these pH ranges deviate significantly from Eq. (6). The $k_{sa,iron}$ at pH 1.7 and 3.8 was 3.58 and 0.42 l/h m^2, which were much higher than predicted by Eq. (6). The results suggest that the effect of EDTA on iron corrosion is minor compared to that of pH as no EDTA was added to the solutions at pH 1.7 and 3.8, whereas solution at pH 10 contained 0.05 M of EDTA.

5.2. TCE degradation

The degradation of TCE by ZVI was observed at initial pH values between 1.7 and 8.0, whereas no TCE reduction was observed at pH 9 and 10. The rates of TCE degradation were higher in the first 24 h of the tests and decreased with time (Fig. 3) with the exception at pH 8.

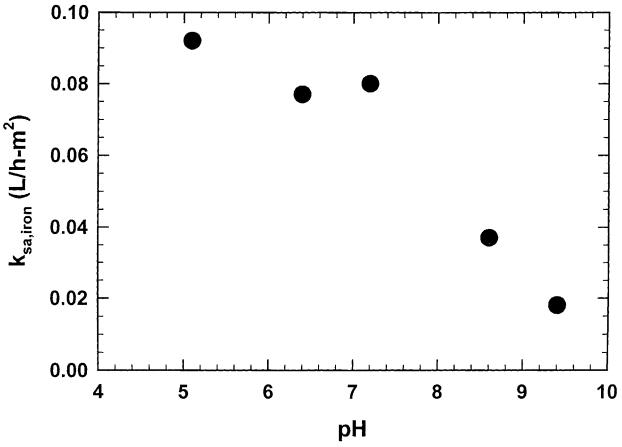

Fig. 2. $k_{sa,iron}$ with pH. The $k_{sa,iron}$ at pH 1.7 and 3.8 (not shown) are 3.58 and 0.42 l/h m^2, respectively.

The degradation rate of TCE at pH 8 appears to be constant. The surface normalized reaction rate constants determined from Eq. (4) shows that the $k_{sa,TCE}$ decreases with pH except at pH 4.9 (Fig. 4 and Table 1). The relationship between $k_{sa,TCE}$ and pH is approximately linear between pH values 3.8 and 8.0. A linear regression between $k_{sa,TCE}$ and pH yields the following equation ($R^2 = 0.83$).

$$k_{sa,TCE} = 0.0844–0.0086\,pH \tag{7}$$

Similar to Eq. (6), Eq. (7) is only valid between pH 3.8 and 8.0. The $k_{sa,TCE}$ at pH 1.7 is more than an order of magnitude higher than that at pH 3.8 and cannot be predicted with Eq. (7), whereas no TCE degradation was observed at initial pH values of 9 and 10. It is

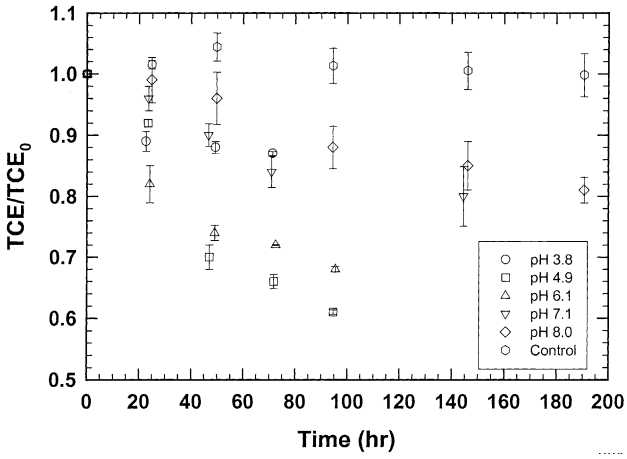

Fig. 3. Ratio of the final to the initial mass of TCE with time at different pH.

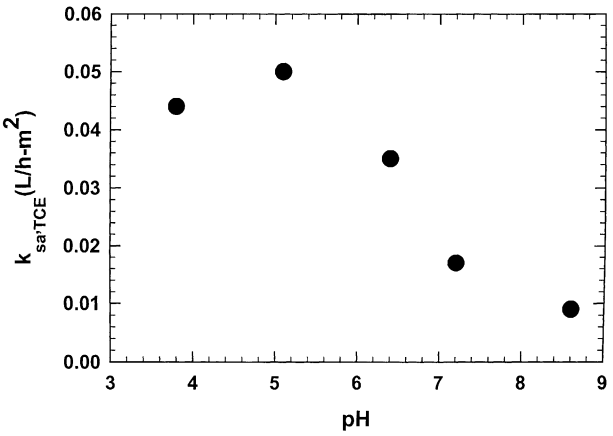

Fig. 4. $k_{sa,TCE}$ with pH. The $k_{sa,TCE}$ at pH 1.7 (not shown) is 0.59 l/h m^2.

worth pointing out that the $k_{sa,TCE}$ at pH 4.9 is slightly higher than at pH 3.8. The reason for this is unclear. However, as the solutions at pH 4.9 contained 0.05 M EDTA and the solution at pH 3.8 contained no EDTA, it is hypothesized that EDTA slightly increased the reaction rate of TCE degradation. In spite of this, the effect of pH on the surface normalized reaction rate constants of TCE is more dominant than the effect of EDTA (Fig. 4).

The $k_{sa,TCE}$ reported in literature ranged from 0.0001 to 0.001 l/h m^2 in unbuffered solutions with a initial pH value of 6.0 [8,13]. In contrast, the $k_{sa,TCE}$ determined at a similar pH value in this study was 30–300 times higher (Table 1). The reason could be that in an unbuffered solution the pH increased rapidly to above 9.0 due to iron corrosion [8], hence resulting in the decrease of rate constants. The other reason that might cause the high values of $k_{sa,TCE}$ is that EDTA was added to prevent iron precipitates from forming in this study. In tests without adding EDTA, the formation of some sort of iron precipitate was evident as indicated by the low total iron concentrations [8,14]. If the ZVI surface was covered with iron precipitate, the transport and adsorption of TCE could be severely impeded, decreasing TCE reaction rate constant. Table 1 also shows that the TCE concentration after 72 h was

Table 1
Summaries of TCE degradation by ZVI at different pH

Initial pH	pH range	$k_{sa,TCE}$ (l/h m^2)	Coefficient of determination	TCE/TCE$_0$ at 72 h	ZVI/ZVI$_0$ at 72 h
1.7	1.7–1.9	0.59	0.87	0.77 at 4.8 h	0.21 at 4.8 h
3.8	3.8–3.8	0.044	0.86	0.87	0.23
4.9	4.9–5.2	0.050	0.93	0.66	0.62
6.1	6.1–6.6	0.035	0.95	0.70	0.65
7.1	7.1–7.3	0.017	0.82	0.84	0.60
8.0	8.0–9.1	0.009	0.86	0.88 at 95 h	0.72 at 95 h

lowest at an initial pH of 4.9. The $C(t)/C_0$ ratio after 72 h at an initial pH of 3.8 was highest at 0.87, although the $k_{sa,TCE}$ at this pH was relatively high. The slow TCE degradation rate is attributed to the fast lost of ZVI due to iron corrosion. Only 23% (weight) of the ZVI remained after 72 h at an initial pH of 3.8 compared to 62% remained at an initial pH of 4.9. The fast loss of ZVI had the most effect on TCE degradation rate at an initial pH of 1.7. The remained ZVI was 21% after 4.8 h and all the ZVI completely reacted after 24 h. Therefore, although at this pH value the $k_{sa,TCE}$ is an order of magnitude higher than that at an initial pH of 4.9 (Table 1), the ratio of $C(t)/C_0$ for TCE remained high at 0.77 after 4.8 h and 0.71 at the end of the test. This suggests that although lowering pH increased the $k_{sa,TCE}$ values, it also caused rapid decrease of ZVI concentration, which is critical in determining the TCE degradation rate. As a result, lowering solution pH values might not be the optimal approach to expedite TCE degradation using ZVI.

The decrease of $k_{sa,TCE}$ with pH suggests techniques that utilize ZVI might loss their effectiveness due to iron corrosion. Recent application of a ZVI reactive barrier (7.9 m in length) showed that pH increased from below 7.0 to as high as 10.4 at the down-gradient end of the barrier [15]. According to the results of this study, the region where the pH is 10.4 has minimal efficiency in degrading TCE. Thus, when designing a ZVI reactive barrier, the buffer capacity of the groundwater is an important factor as it affects the pH profiles in the barrier.

5.2.1. Effects of head space

The experiments in this study were conducted with 6.0 ml of headspace. As the reaction of iron corrosion generated hydrogen gas, the amount of head space affected the pressure inside the reactor and hence, could affect the reaction rate. The effect was investigated by determining the k_{sa} of TCE and ZVI at an initial pH of 6.1 under head space of 0, 6.0, and 10.0 ml, respectively. The results indicate that the k_{sa} of TCE and ZVI increased by 2-folds when the head space was increased from zero to 6.0 ml, whereas there was insignificant change between a head space of 6.0 and 10.0 ml (Table 2).

The results in Table 2 indicate that the amount of hydrogen gas on the ZVE surface may affect $k_{sa,TCE}$ and $k_{sa,iron}$. Under the condition of zero head space, we observed hydrogen gas bubbles forming and staying on the surface of ZVI. Under 6 ml of head space, hydrogen gas bubbles formed on the ZVI surface and escaped to the head space once the bubbles reached certain sizes. The headspace in most applications using ZVI as a reductant, such as in a reactive containment wall for a TCE plume, is the atmosphere. Hence, the results in Table 2 suggest that $k_{sa,TCE}$ obtained from zero head space experiments may underestimate the degradation rate of TCE in field applications.

Table 2
Surface normalized reaction rate constants at pH 6.1 with different head space

Head space (ml)	$k_{sa,TCE}$ (l/h m^2)	$k_{sa,iron}$ (l/h m^2)
0	0.018	0.028
6.0	0.035	0.051
10.0	0.035	0.055

5.2.2. Head space pressure

The head space pressure was measured to monitor the generation of hydrogen gas by iron corrosion. It is assumed that the partial pressure of ethene and ethane (Eq. (1)) was negligible compared to that of the hydrogen gas as the moles of ZVI was 90 times that of TCE. Even if all the TCE was reduced, it only consumed 3 wt.% of the ZVI added. Therefore, the total moles of hydrogen gas produced in a reactor can be determined by calculating the moles of ferrous ions in the solution as 1 mol of ZVI is consumed, 1 mol of hydrogen gas is generated (Eq. (3)).

The hydrogen gas produced can enter the gaseous, aqueous, and solid phases [16]. The moles of hydrogen gas in the gaseous phase can be determined using the measured head space pressure according to Eq. (8).

$$H_2(g) = \frac{P_{H_2} V_{hs}}{8314T} \tag{8}$$

where P_{H_2} = the partial pressure (kPa) of hydrogen in the reactor, which equals the measured pressure minus the vapor pressure of water (3.167 kPa at 25°C), V_{hs} = the volume of head space (ml), and T = the temperature (K). The moles of hydrogen gas in the aqueous phase are governed by the hydrogen solubility in water and can be calculated according to Eq. (9) [16].

$$H_2(aq) = 7.515 \times 10^{-6} P_{H_2} M_{H_2O} \tag{9}$$

where M_{H_2O} = the mass of test solution (kg). The uptake of hydrogen gas by the solid increases with the partial pressure of hydrogen [16]. The mechanism of the hydrogen gas entering the iron solid is not well understood. It has been proposed that hydrogen gas bonds at sites within the iron lattice and microfractures at the surface and migrate through the lattice and accumulate at sites of impurities and grain boundaries [17]. In addition, we observed micro-bubbles of hydrogen gas forming on the surface of ZVI during the test. This fraction of hydrogen gas cannot be estimated with any of the above methods. Thus, as the hydrogen bubbles accumulated on the ZVI surface, it was considered part of the hydrogen gas that partitioned in the solid phase in this study.

The total amount of hydrogen gas in the aqueous and gaseous phases in the reactors at a specific head space pressure was determined by summing the results of Eqs. (8) and (9). The amount of hydrogen gas in the solid phase was obtained by subtracting the hydrogen gas in the aqueous and gaseous phases from the total produced. The percentage of hydrogen gas in solid phase decreases with head space pressure (Fig. 5). The data in Fig. 5 includes the results of tests conducted at different pH values. It indicates that as high as 80% of hydrogen gas was in the solid phase when the head space pressure was low. This suggests that most of the hydrogen gas generated at the beginning of the test either formed micro-bubbles at the ZVI surface or was absorbed by the ZVI. As the head space pressure increases, more hydrogen gas partitioned into the aqueous and gaseous phases. The percentage of hydrogen gas in the solid phase seemed stabilized between 22 and 32% when the head space pressure was above 160 kPa (Fig. 5). The formation of bubbles of hydrogen gas on the ZVI surface might affect the TCE degradation in two ways. First, it could hinder the transport and diffusion of TCE from the solution to the ZVI surface and vice versa for the TCE degradation products. As a result, it decreases the degradation rate of TCE. Secondly, the hydrogen gas could

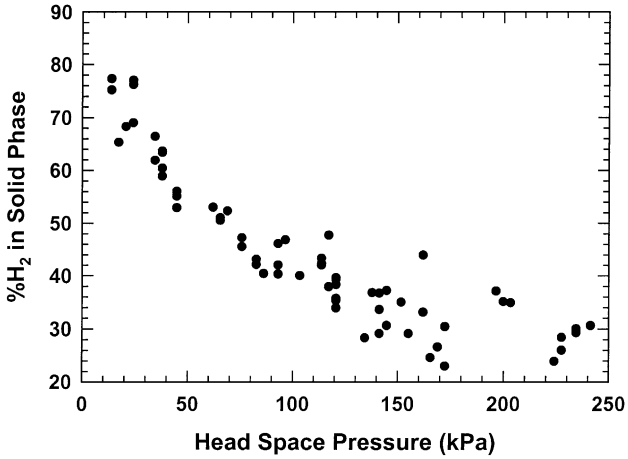

Fig. 5. Percentage of hydrogen gas in the solid phase as a function of head space pressure. Hydrogen gas in the solid phase includes hydrogen gas sorbed by the ZVI and hydrogen gas that formed bubbles on the surface of ZVI.

serve as an electron donor for TCE reduction, resulting in higher TCE degradation rate [2]. According to the tests conducted at different head spaces (Table 2), the hydrogen gas bubbles on ZVI is detrimental to the TCE degradation rate, suggesting the first effect is more dominant.

6. Conclusions

The surface normalized reaction rate constant of TCE degradation and iron corrosion using ZVI decreases with pH. Although lowering solution pH increases the degradation rate constant of TCE, it also expedites the disappearance of ZVI by iron corrosion. As the degradation rate of TCE is proportional to the surface area of ZVI, the TCE degradation rate at low pH is not necessarily higher than at higher pH providing that the amount of ZVI is limited. For the pH range tested in this study (1.7–10.0), the TCE degradation rate at pH 4.9 is highest.

The $k_{sa,TCE}$ measured was 30–300 times higher than that in the literature at an initial pH of 6. The difference can be attributed to the pH effects and the precipitation of ferrous hydroxide on the surface of ZVI. The pH effect was clearly demonstrated in this study as EDTA was added to prevent ferrous ions from precipitating. The effect of ferrous hydroxide precipitation on TCE degradation rate is not well understood and further researches are needed to characterize the effect. The addition of EDTA appeared to slightly increase the surface normalized reaction rate constant. However, this effect is insignificant when compared to the effect of pH.

Formation of hydrogen gas bubbles on the surface of ZVI may decrease the $k_{sa,TCE}$ buy hindering the transport of TCE and degradation products between the solution and reaction

sites on ZVI. Therefore, if a contaminated aquifer is unconfined, using $k_{sa,TCE}$ obtained under zero head space might underestimate the degradation rate of TCE by ZVI.

Acknowledgements

This research was supported in part by an appointment to the Postgraduate Research Program at the National Risk Management Research Laboratory, administered by the Oak Ridge Institute for Science and Education through an interagency agreement between the US Department of Energy and the US Environmental Protection Agency. Although the research in this paper has been conducted in the US Environmental Protection Agency, it does not necessarily reflect the views of the Agency. Mention of trade names or commercial products does not constitute endorsement or recommendation for use.

References

[1] R.W. Gillham, S.F. O'Hannesin, Ground Water 6 (1994) 958–967.
[2] L.J. Matheson, P.G. Tratnyek, Environ. Sci. Technol. 28 (1994) 2045–2053.
[3] R. Muftikian, Q. Fernando, N. Korte, Water Res. 29 (1995) 2434–2439.
[4] C. Grittini, M. Malcomson, N. Korte, Environ. Sci. Technol. 29 (1995) 2898–2900.
[5] I.F. Cheng, Q. Fernando, N. Korte, Environ. Sci. Technol. 31 (1997) 1074–1078.
[6] B. Deng, D. R Burris, T.J. Campbell, Environ. Sci. Technol. 33 (1999) 2651–2656.
[7] S.F. O'Hannesin, R.W. Gillham, Ground Water 36 (1998) 164–170.
[8] C. Su, R.W. Puls, Environ. Sci. Technol. 33 (1999) 163–168.
[9] M.M. Scherer, B.A. Balko, D.A. Gallagher, P.G. Tratnyek, Environ. Sci. Technol. 32 (1998) 3026–3033.
[10] M.M. Scherer, B.A. Balko, P.G. Tratnyek, in: D.L. Sparks, T. Grundl (Eds.), Mineral–Water Interfacial Reactions: Kinetics and Mechanisms, ACS Symposium no. 715, American Chemical Society, Washington, DC, 1998.
[11] D.R. Burris, T.J. Campbell, V.S. Manoranjan, Environ. Sci. Technol. 29 (1995) 2850–2855.
[12] W.D. Schecher, D.C. McAvoy, Mineql+ Chemical Equilibrium Modeling System, Environmental Research Software, Hallowell, ME, 1998, 318 pp.
[13] T.L. Johnson, M.M. Scherer, P.G. Tratnyek, Environ. Sci. Technol. 30 (1996) 2634–2640.
[14] W.S. Orth, R. W Gillham, Environ. Sci. Technol. 30 (1996) 66–71.
[15] D.H. Phillips, B. Gu, D.B. Watso, Y. Roh, L. Liang, S.Y. Lee, Environ. Sci. Tchhnol. 34 (2000) 4169–4176.
[16] E.J. Reardon, Environ. Sci. Technol. 29 (1995) 2936–2945.
[17] A. Gourmelon, Mem. Sci. Rev. Metall. 72 (1975) 475–489.